Effect of structural arrest on Poisson's ratio in nanoreinforced elastomers

C. G. Robertson,[1] R. Bogoslovov,[2] and C. M. Roland[2]
[1]*Center for Research and Technology, Bridgestone Americas, 1200 Firestone Parkway, Akron, Ohio 44317-0001, USA*
[2]*Chemistry Division, Code 6120, Naval Research Laboratory, Washington, D.C. 20375-5342, USA*
(Received 27 November 2006; published 9 May 2007)

We evaluate the strain amplitude (γ) dependence of the dynamic storage and loss moduli for polybutadiene elastomers containing carbon black particles of varied size at a constant volume fraction of 0.18. Measurements of the low-strain hysteretic softening (Payne effect or unjamming transition) in both shear and uniaxial extension modes allow the γ dependence of Poisson's ratio (ν) to be determined. For elastomers with a fully agglomerated filler network, the breakup of the jammed state with increasing strain induces a transition from $\nu \sim 0.35$ to the limiting value for an incompressible material, $\nu=0.5$. This transition is more marked for samples containing smaller filler particles. The effect is similar to the change caused by temperature in the glass transition zone of amorphous polymers, reflecting the parallel between deformation in jammed systems and temperature (and the volume changes associated with it) in glasses; thus, the Payne effect resembles the glass transition in polymers and molecular liquids. We also show herein that the alleviation of structural arrest in filled rubber occurs at a constant value of strain energy, independent of the size of the reinforcing particles or the nature of the strain (shear vs tension). Contrary to the results for shear or tensile deformation, under hydrostatic pressure (volumetric strain) a value of $\nu=0.5$ is maintained for all magnitudes of strain. Along with the absence of hysteresis in cyclic pressure-volume measurements, this demonstrates the distinct behavior of the filler network for hydrostatic compression, in which there is no relative displacement of polymer and filler.

DOI: 10.1103/PhysRevE.75.051403 PACS number(s): 83.80.Hj, 64.70.Dv, 81.05.Qk

INTRODUCTION

One of the defining characteristics of particle-filled elastomers is the strong reduction in the storage modulus (G') and the appearance of a peak in the loss modulus (G''), which occur with increasing dynamic strain amplitude (γ). This behavior is commonly called the Payne effect [1,2], or alternatively the Fletcher-Gent effect [3]. (The term "Mullins softening" is sometimes used interchangeably with the Payne effect, but the former is a different phenomenon that occurs at larger strains [4].) The Payne effect is an unusual type of nonlinear viscoelasticity. For unfilled polymers at temperatures well above the glass transition, nonlinear effects are not observed until ca. $\gamma > 0.5$, yet carbon black, silica, or other nanoreinforcing particles induce significant strain softening in the small-strain region ($0.001 \leqslant \gamma \leqslant 0.1$). Another unusual feature of the Payne effect is that the sinusoidal response lacks higher-order harmonics [5–7]; the nonlinearity is only observed as a change in the ratio of stress to strain upon change in amplitude of either variable.

Various models have been proposed to describe the Payne effect. Kraus [8] ascribed the phenomenon to the dynamic breaking and reforming of filler-filler contacts during an oscillatory deformation. Although phenomenological, the Kraus model was the first to offer a quantitative description of the Payne effect. Another model is due to Maier and Göritz [9], who emphasized the role of polymer debonding from the surface of filler particles. These and other models have been reviewed by Heinrich and Klüppel [5]. Two more recent approaches consider the strain softening of the "glassy" shell of polymer surrounding filler particles [10] and the strain dependence of polymer-filler interactions and associated trapped entanglements [11]. These concepts appear less generally satisfactory compared to the conventional idea of filler networking [8,12,13]. An agglomerated filler network also accounts for the electrical properties and their strain dependence in rubber containing carbon black [14–16]. A new concept proposed by Robertson and Wang [7,17,18] is the view that the Payne effect is a jamming-unjamming transition, in which the role of strain is analogous to the effect of temperature on glass-forming materials.

Elastomers are generally considered to be practically incompressible with a value of Poisson's ratio (ν) nearly equal to 0.5. Poisson's ratio depends on the chemical structure of the elastomer and on the filler concentration, but these dependences are very weak. A variation in the range from 0.494 to 0.5 was found for ν for a variety of polymer networks and a broad range of carbon black content [19]. However, even a slight deviation from $\nu=0.5$ can have a significant effect on mechanical behavior [20,21]. The dependence on strain of Poisson's ratio has been interpreted in terms of filler-elastomer dewetting and vacuole formation [22,23]. However, these effects are limited to relatively large filler particles that interact poorly with the polymer; generally, hydrocarbon elastomers reinforced with carbon black do not exhibit this behavior.

Aside from the special case of vacuole formation in poorly reinforced rubber, the effect of strain on Poisson's ratio in filled elastomers has not been studied heretofore, particularly in the small-oscillatory-strain region where the Payne effect is manifested. Indeed, ν is usually determined from measurements of the static Young's modulus (E) and bulk modulus (K), rather than from dynamic moduli. In this work we use oscillatory shear, oscillatory tension and compression, and hydrostatic pressure-volume measurements to quantify the strain-dependent changes in Poisson's ratio and their relationship to the Payne effect.

EXPERIMENT

The polymer used herein was a commercial polybutadiene (Diene 40NF from Firestone Polymers) for which M_w =192 kg/mol, M_w/M_n=2.01, and T_g=−93 °C. It is a random terpolymer of 38% *cis*-1,4, 51% *trans*-1,4, and 11% 1,2 (vinyl) butadiene units. The carbon blacks (from Sid Richardson Carbon Co.) were ASTM N110, N220, N339, N351, N550, N660, and N762. The rubber formulation was maintained constant, except for the carbon black type: 100 parts (weight basis) polymer, 50 parts carbon black (volume fraction=0.18), 15 parts aromatic oil, 3 parts zinc oxide, 0.95 parts antioxidant, 2 parts hydrocarbon resin, 1 part wax, and 2 parts of stearic acid, with 1.3 parts sulfur, 1.4 cyclohexylbenzothiazole sulfenamide, and 0.2 diphenylguanidine as the curatives. A "gum" polybutadiene sample, lacking filler but otherwise identical, was also prepared. Mixing was carried out in a Brabender Plasticorder (5 min.; 60 rpm; initial T=110 °C; end T=150 °C), followed by incorporation of the curatives (1.5 min.; 60 rpm; initial T=70 °C; end T=110 °C). This material was then mixed at 60 °C on a two-roll mill. Cylinders (length=15.5 mm, diameter =9.4 mm) and sheets (15.2 cm×15.2 cm×2.5 mm; 15.2 cm×15.2 cm×1.9 mm) were cured by molding under pressure at 165 °C for 20 min.

Viscosities were measured at 130 °C in a Mooney viscometer using the large rotor. Stress-strain curves were obtained on ring samples (ASTM D412) with an Instron Universal Testing Machine at 23 °C and an engineering strain rate of 0.33 s^{-1}. Carbon black macrodispersion was determined with a Federal Products Surfanalyzer 2000, a surface profilometer calibrated with dispersion results from microscopy. The dispersion number from this test refers to the percentage of particle agglomerates smaller than 5 μm. Bound rubber (defined as the percentage of polymer not extracted by solvent from the uncured rubber) was measured by immersion in an excess of toluene at 23 °C for three days, followed by filtering, drying, and weighing.

For oscillatory shear tests, a ring sample (inner and outer diameters 16.2 and 18 mm, respectively) was cut from the cured 2.5-mm-thick sheet, then glued between parallel plates. The ratio of the strain at the outer edge to that at the inner for this geometry is 1:10; hence, the strain can be considered as essentially constant over the test piece. A Rheometrics ARES was used for the dynamic shear measurements, with the strain amplitude systematically increased (except where noted). Dynamic tension and compression measurements (mean strain zero) were carried out on an IMass Dynastat Mark II, operated in displacement control. The cylindrical test specimens (height 15.5 mm and diameter 9.4 mm) were glued to the test fixtures. This geometry minimizes shearing at the bonded surfaces and the data herein are presented without correction for "barreling" (deviation from a right circular cylinder). Both the shear and extension measurements were done at 23 °C using a frequency of 3.14 rad/s (0.5 Hz). The average rate at which the strain was changed, which can influence the observed Payne effect, was ~0.004 decades of γ per second.

For pressure-volume-temperature (PVT) measurement, a Gnomix instrument [24] was used. The method employs mercury as a confining fluid, with the sample maintained in a flexible bellows. The change in length of the bellows is monitored magnetically. Pressure was increased isothermally at a rate of 4.9 kPa/s up to 200 MPa and then reduced at the same rate; the entire measurement took about one day. The density at ambient conditions was measured by the buoyancy method in order to convert relative changes in V to specific volumes.

TABLE I. Characteristics of carbon blacks.

Carbon black type	d (nm)[a]	D (nm)[a]	Iodine number (g/kg)[b,c]	DBP absorption (ml/100 g)[b,d]
N110	17±7	54±26	145	113
N220	21±9	65±30	121	114
N339	26±11	75±34	90	120
N351	31±14	89±47	68	120
N550	53±28	139±71	43	121
N660	63±36	145±74	36	90
N762	110±53	188±102	27	65

[a]Primary particle diameter d and particle aggregate diameter D from Hess and McDonald [25].
[b]Sid Richardson Carbon Company data [43].
[c]Indicator of carbon black particle size (inversely related to D); ASTM D1510.
[d]Indicator of carbon black structure; ASTM D2414.

RESULTS AND DISCUSSION

Filler characteristics

The carbon blacks and their properties are listed in Table I. Carbon black fillers are composed of roughly spherical particles strongly fused together in the manufacturing process to form aggregates. Both the aggregate diameter D and the primary particle diameter d increase systematically in the series of fillers used herein. A related (but inverse) size metric is the iodine number. The term "structure" refers to the shape of the aggregates, with higher-structure carbon blacks having more surface area due to branching. A common indicator of structure is the *n*-dibutyl phthalate (DBP) absorption, which can be related to the number of particles comprising an aggregate [26]. The majority of our experiments involved polybutadiene containing N110, N220, N339, and N660 carbon blacks. As seen in Table I, the structure of these four fillers is fairly constant. Thus, these rubbers were essentially identical with the exception of the average size of the filler particles. Smaller particles result in more bound rubber, a higher viscosity for the uncured compounds, and better reinforcement (especially apparent in ultimate tensile properties) of the cross-linked elastomers. These properties are listed in Table II.

Agglomeration of microdispersed carbon black aggregates within an elastomeric matrix leads to formation of a percolated filler network, which we consider as the primary origin of the Payne effect. Poor mixing can obscure the relationship between the filler characteristics and the network structure. Good "macrodispersion" was achieved herein, as

TABLE II. Properties of uncured and vulcanized rubbers.

Carbon black type	Bound rubber (%)	Macrodispersion[a] (%)	Mooney viscosity[b]	100% secant modulus[d] (MPa)	Stress at break[d] (MPa)	Elongation at break[d] (%)
Unfilled			14.4[c]			
N110	17.2	98.3	45.1	1.50	12.9	605
N220	15.9	97.9	42.6	1.52	12.4	549
N339	15.4	97.3	39.4	1.47	11.5	516
N351	14.9	97.6	36.7	1.44	10.1	498
N550	7.3	99.0	33.4	1.41	10.8	505
N660	5.6	96.8	29.7	1.25	9.9	524
N762	~0	99.8	26.3	1.11	6.1	445

[a]Percentage of carbon black agglomerates smaller than 5 μm.
[b]Mooney viscosity (relative value of η) of uncured compound at 130 °C.
[c]Value used for $\eta(0)$ in Eq. (1).
[d]Measured in tension at 23 °C and strain rate of 0.33 s^{-1}.

evidenced by the high concentration of agglomerates smaller than 5 μm (Table II).

Although the carbon black concentration was held constant at a volume fraction of 0.18, the different particle sizes, and hence different surface areas, give rise to variations in the effective filler loadings. The structure of the carbon black particles occludes some of the rubber; that is, polymer chains are immobilized by virtue of their presence in the void space within the aggregates [27]. These chains are constrained and isolated from the stress field, and thus act more as a filler than a deformable polymer. The contribution of occluded rubber is seen directly in the increase of the Mooney viscosity (Table II) with particle size. Applying the Einstein viscosity equation

$$\eta(\phi) = \eta(0)(1 + 2.5\phi), \tag{1}$$

the effective volume fraction of filler, ϕ, can be determined, with the occluded rubber volume fraction (ϕ_{occ}) equal to $\phi - 0.18$, where 0.18 is the volume fraction of filler in the rubber. These results are plotted in Fig. 1, showing the bound rubber (Table I) as a function of the occluded rubber (expressed as a percentage rather than a fraction). There is the expected strong increase in ϕ_{occ} with decreasing particle size. This anticipates a concomitant increase in the magnitude of the Payne effect, as described below.

Payne effect and poisson's ratio

The shear modulus (G) and tensile modulus (E) are related by Poisson's ratio according to

$$E = 2G(1 + \nu). \tag{2}$$

For dynamic measurements on viscoelastic materials, we substitute the corresponding complex quantities E^* and G^* [28]. For the compounds herein, the loss factors were sufficiently low that the storage moduli were used for the calculation:

$$E' = 2G'(1 + \nu). \tag{3}$$

The usual assumption is that rubbers are essentially incompressible ($\nu \approx 0.5$), so that $G' \sim E'/3$. These quantities are plotted versus strain amplitude in Fig. 2 for the four cured samples. It is evident that the Payne effect is diminished with increasing particle size. From these data we calculate Poisson's ratio from Eq. (3), and the resulting γ-dependent ν are plotted in Fig. 3. At large strain $\nu = 0.5$, decreasing to a value ~0.35 at low γ (except for the polybutadiene with N660). For the larger-particle N660 the agglomerate network is less well developed; thus, the Payne effect is weaker and the low-strain diminution of Poisson's ratio is reduced. This difference between a well-developed filler network (N110) and a weakly agglomerated filler (N660) is emphasized in Fig. 4.

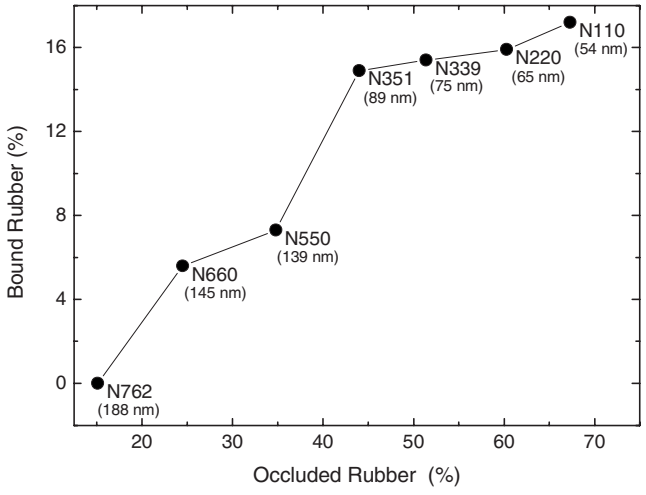

FIG. 1. Bound rubber as a function of the occluded rubber calculated using Eq. (1) for polybutadiene having 18% by volume of the indicated carbon black type. The values are plotted here as percentages instead of fractions. The numbers in parentheses are the average values of particle aggregate diameter (D) for each carbon black (Table I).

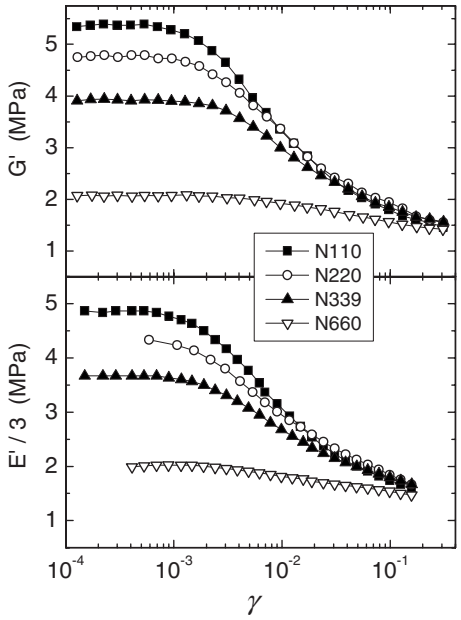

FIG. 2. Dynamic shear and tensile storage moduli (the latter divided by 3) vs strain amplitude at 23 °C and 0.5 Hz for polybutadiene having 0.18 volume fraction of the indicated carbon black.

For the N110-filled elastomer Poisson's ratio was also determined from the bulk modulus, $K = -V(dP/dV)|_T$, measured by hydrostatic compression. The inset to Fig. 5 shows the isothermal specific volume measured as a function of pressure at $T=25.9$ °C. (The specific volume at ambient pressure was measured independently; $V_0=0.9239$ ml^3/g at this temperature.) Invariably there is hysteresis when the Payne effect is cyclically measured with increasing then decreasing strain amplitude. This is ascribed to the slow recovery of the filler network, disrupted by larger deformation. An example is shown in Fig. 6 for the elastomer with the N110 carbon black. This behavior is quite different from the response to a reversing pressure in the hydrostatic compression experiment (Fig. 5 inset), for which V is path independent, being the same at a given pressure attained by either increasing or decreasing P. The slow rate of pressure variation (4.9 kPa/s) would allow for some recovery during this measurement, but the dominant effect is a lack of disruption of the network structure. The obvious difference between the oscillatory measurements and the volumetric experiment is the absence of relative displacements of filler and polymer in the latter.

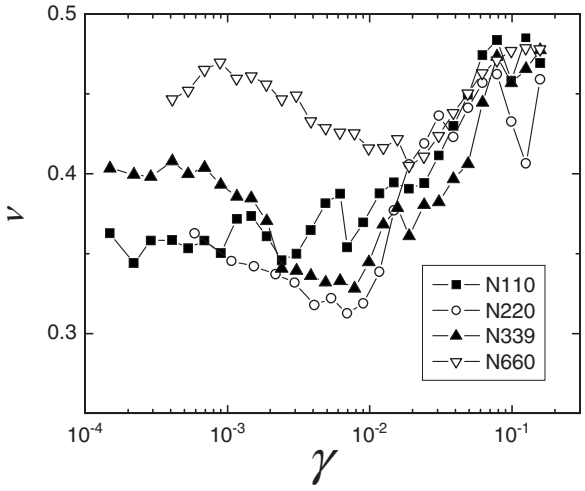

FIG. 3. Variation of Poisson's ratio with strain amplitude for filled polybutadiene rubbers.

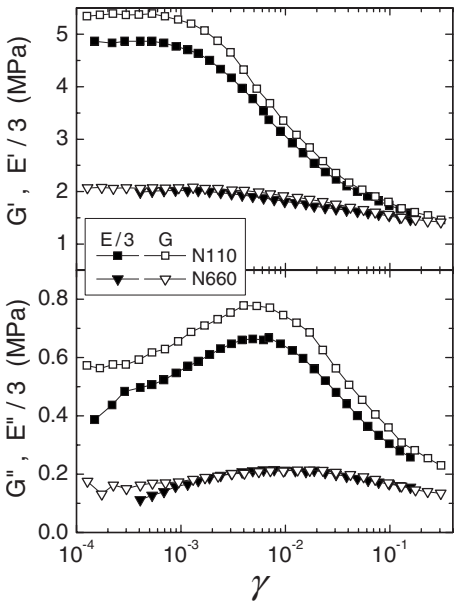

FIG. 4. Dynamic shear and tensile moduli (the latter divided by 3) vs. strain at 23 °C and 0.5 Hz for polybutadiene containing 0.18 volume fraction of N110 carbon black (having a well-developed filler network) and N660 carbon black (weakly agglomerated filler).

The P-V data for the filled rubber conformed well to the Tait equation of state [24], commonly applied to neat (unfilled) polymers and molecular liquids. At fixed T

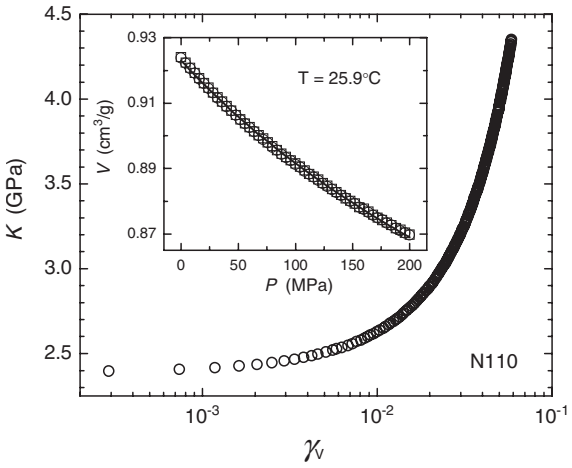

FIG. 5. Bulk modulus as a function of volumetric strain for polybutadiene with 0.18 volume fraction of N110 carbon black. Inset shows the pressure-volume data (only every fifth point shown for clarity) measured at 25.9 °C for conditions of increasing P (□) followed by decreasing P (○). The solid line is the fit to Eq. (4) with $V_0=0.9239$ ml/g and $B=209.8$ MPa.

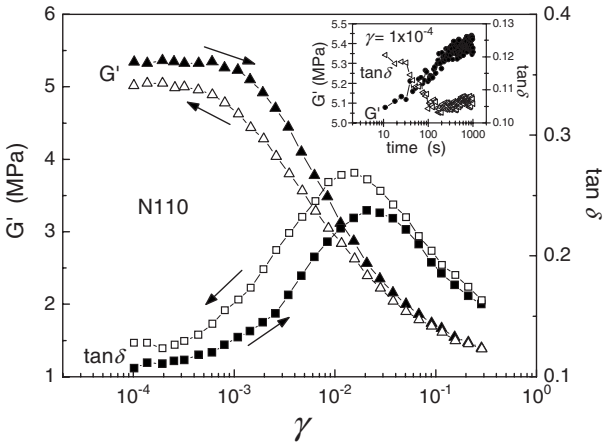

FIG. 6. Oscillatory shear storage modulus and loss tangent for polybutadiene containing N110 carbon black. The strain amplitude was increased and then decreased, in the direction indicated by the arrows. The inset shows the time-dependent recovery of G' and the loss tangent after the strain was reduced to $\gamma=1\times10^{-4}$.

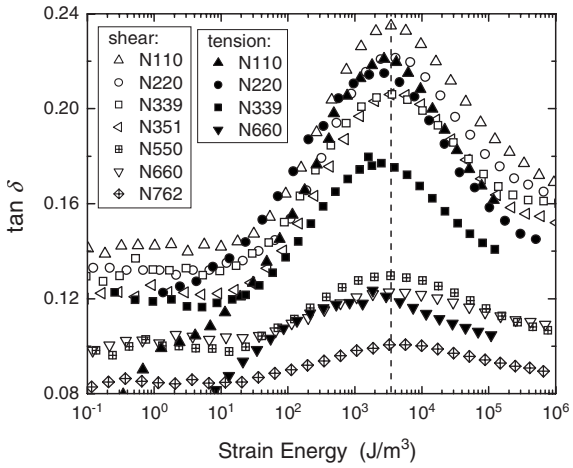

FIG. 7. Loss tangent vs strain energy for polybutadiene with the indicated carbon black. The vertical dashed line denotes the characteristic strain energy (=3.5 kJ/m^3, independent of filler size and approximately independent of strain mode) associated with breakup of the filler network.

$$V(P) = V_0\left[1 - 0.0894\ \ln\left(1 + \frac{P}{B}\right)\right]. \tag{4}$$

The data in Fig. 5 were fitted using $B=209.8$ MPa. From Eq. (4) the bulk modulus is [29]

$$K = \frac{(B+P)V}{0.0894V_0}. \tag{5}$$

This quantity is plotted in Fig. 5 vs the volumetric strain $\gamma_V=dV/V_0$. In distinction to the response to shear or tensile deformation, increasing pressure does not soften the filled rubber; rather the bulk modulus increases with increasing hydrostatic strain in the same manner observed for unfilled polymers [24]. In the low-pressure limit $K=2.39\pm0.04$ GPa. Poisson's ratio is related to the various moduli as

$$\nu = \frac{3K-2G}{6K+2G} = \frac{3K-E}{6K}. \tag{6}$$

We calculate $\nu=0.50$ at low (volumetric) strain, which is substantially larger than the low-strain value from oscillatory shear and tension measurements (Fig. 2).

From published PVT data on an unfilled and uncured polybutadiene of similar chemical structure [24], we calculate $K=2.1$ GPa at ambient T, which is smaller than the bulk modulus measured herein for the filled polybutadiene rubber. It would be of interest to compare in more detail the compressibility and its pressure dependence for rubbers with and without reinforcing filler. Such information can provide insight into how stress distributes in the polymer and filler network in response to hydrostatic loading.

Finally we assess a recently discovered correlation between the Payne effect and the dynamic strain energy: for different concentrations of filler and different test frequencies, the disruption of the agglomerate network transpired at the same value of the shear strain energy [18]. This isoenergetic nature of unjamming was first demonstrated for a variety of particle-filled materials [17]. In Fig. 7 the loss tangent measured in both shear and tension is plotted as a function of the strain energy, the latter given by the product of the strain amplitude and the in-phase stress. The dejamming transition, reflected in the maximum in the loss tangent, is associated with a characteristic value of the dynamic strain energy, independent of carbon black type and, to a lesser degree, of mode of deformation. This extension of the isoenergetic nature of the Payne effect to different fillers and different strain modes shows the generality of the phenomenon.

FINAL REMARKS

Colloids and granular solids can be considered structurally arrested systems that can be "unjammed" by application of deformation, such as vibration or mechanical strain. The Payne effect in filled rubber represents such an unjamming process. The concept of "effective temperature" has been proposed to explain similarities between deformation in jammed heterogeneous materials and temperature in traditional glasses [30–37], and this analogy has been extended to the Payne effect in particle-filled elastomers [7,17,18]. The increase observed herein in the value of Poisson's ratio with increasing γ is similar to the transition in ν seen in amorphous polymers upon heating through their glass transition temperature [38,39]. This is illustrated in Fig. 8 with results from Kono [38] for the temperature dependence of ν for polystyrene and poly(methyl methacrylate). These results are qualitatively similar to the γ-dependent transition seen in Figs. 3 and 4 for the carbon-black-filled polybutadienes. The effect of strain on structural arrest in the latter mimics the role of temperature in vitrifying materials.

Of course, a direct analogy between the Payne effect and the glass transition has its limitations. The two phenomena involve different molecular mechanisms and different length scales. Moreover, the temperature dependence of the dynamics of glass-forming liquids and polymers does not reflect a thermally activated process. As temperature is varied, the

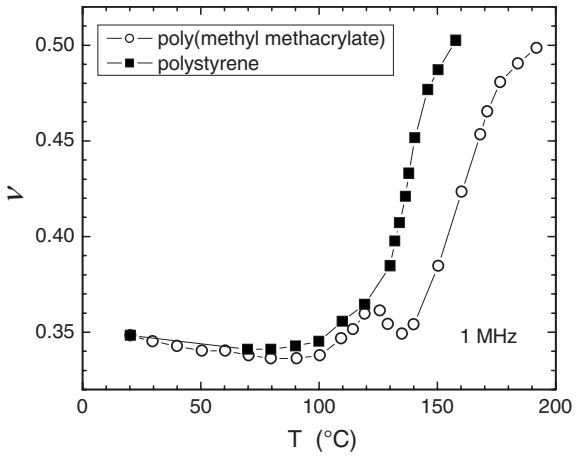

FIG. 8. Temperature dependence of Poisson's ratio for two amorphous polymers from Kono [38].

volume changes, and both thermal energy and volume govern the temperature dependence [40,41]. The structural arrest of filled rubber, for which strain energy appears to be the dominant control variable (Fig. 7), has a more direct connection to colloidal glasses [42]. Certainly continuing efforts to identify physical parallels between these different classes of mobility-frustrated systems are necessary to achieve a universal understanding of glasses and jammed particle systems.

Distinct from the effect of mechanical strain, hydrostatic compression has minimal effect on the filler network. At low volumetric strains the magnitude of the bulk modulus is consistent with the value of $\nu=0.5$ achieved only for high shearing or tensile strains. Moreover, the bulk data lack the hysteresis associated with breakup and recovery of an agglomerate network. It is surprising that $\nu=0.5$ even though hydrostatic pressure does not disrupt the filler network; that is, the material response is that of an unjammed system. Clearly, Poisson's ratio of particle-filled polymers is a complex material function of both the extent and type of deformation.

ACKNOWLEDGMENTS

The work at the Naval Research Laboratory was supported by the Office of Naval Research. C.G.R. thanks Bridgestone Americas for permission to publish, and R.B. thanks the American Society for Engineering Education for financial support.

[1] A. R. Payne, J. Appl. Polym. Sci. **3**, 127 (1960).
[2] A. R. Payne, J. Appl. Polym. Sci. **6**, 57 (1962).
[3] W. P. Fletcher and A. N. Gent, Trans. Inst. Rub. Ind. **29**, 266 (1953).
[4] C. M. Roland, Rubber Chem. Technol. **33**, 659 (1989).
[5] G. Heinrich and M. Klüppel, Adv. Polym. Sci. **160**, 1 (2002).
[6] L. Chazeau, J. D. Brown, L. C. Yanyo, and S. S. Sternstein, Polym. Compos. **21**, 202 (2000).
[7] C. G. Robertson and X. Wang, Europhys. Lett. **76**, 278 (2006).
[8] G. Kraus, J. Appl. Polym. Sci.: Appl. Polym. Symp. **39**, 75 (1984).
[9] P. G. Maier and D. Göritz, Kautsch. Gummi Kunstst. **49**, 18 (1996).
[10] H. Montes, L. Lequeux, and J. Berriot, Macromolecules **36**, 8107 (2003).
[11] S. S. Sternstein and A.-J. Zhu, Macromolecules **35**, 7262 (2002).
[12] A. I. Medalia, Rubber Chem. Technol. **47**, 437 (1974); **51**, 411 (1978).
[13] Z. Zhu, T. Thompson, S.-Q. Wang, E. D. von Meerwall, and A. Halasa, Macromolecules **38**, 8816 (2005).
[14] A. R. Payne, J. Appl. Polym. Sci. **9**, 1073 (1965).
[15] B. B. Boonstra, Rubber Chem. Technol. **50**, 194 (1977).
[16] C. M. Roland, C. G. Robertson, L. Nikiel, and J. E. Puskas, Rubber Chem. Technol. **77**, 372 (2004).
[17] C. G. Robertson and X. Wang, Phys. Rev. Lett. **95**, 075703 (2005).
[18] X. Wang and C. G. Robertson, Phys. Rev. E **72**, 031406 (2005).
[19] B. P. Holownia, Rubber Chem. Technol. **48**, 246 (1975).
[20] M. A. Anderson, P. H. Mott, and C. M. Roland, Rubber Chem. Technol. **77**, 293 (2004).
[21] A. N. Gent and Y.-C. Hwang, Rubber Chem. Technol. **61**, 630 (1988).
[22] T. L. Smith, Trans. Soc. Rheol. **3**, 113 (1959).
[23] R. J. Farris, J. Appl. Polym. Sci. **8**, 25 (1964).
[24] P. Zoller and D. J. Walsh, *Standard Pressure-Volume-Temperature Data for Polymers* (Technomic, Lancaster, PA, 1995).
[25] W. M. Hess and G. C. McDonald, Rubber Chem. Technol. **56**, 892 (1983).
[26] A. I. Medalia, J. Colloid Interface Sci. **32**, 115 (1970).
[27] A. I. Medalia, Rubber Chem. Technol. **45**, 1171 (1972).
[28] N. W. Tschoegl, W. G. Knauss, and I. Emri, Mech. Time-Depend. Mater. **6**, 3 (2002).
[29] B. Hartmann, G. F. Yee, and E. Balizer, J. Acoust. Soc. Am. **108**, 65 (2000).
[30] *Jamming and Rheology: Constrained Dynamics on Microscopic and Macroscopic Scales*, edited by A. J. Liu and S. R. Nagel (Taylor and Francis, New York, 2001).
[31] G. D'Anna, P. Mayor, A. Barrat, V. Loreto, and F. Nori, Nature (London) **424**, 909 (2003).
[32] L. Berthier and J. L. Barrat, J. Chem. Phys. **116**, 6228 (2002).
[33] I. K. Ono, C. S. O'Hern, D. J. Durian, S. A. Langer, A. J. Liu, and S. R. Nagel, Phys. Rev. Lett. **89**, 095703 (2002).
[34] P. Sollich, F. Lequeux, P. Hebraud, and M. E. Cates, Phys. Rev. Lett. **78**, 2020 (1997).
[35] C. Song, P. Wang, and H. A. Makse, Proc. Natl. Acad. Sci. U.S.A. **102**, 2299 (2005).
[36] H. A. Makse and J. Kurchan, Nature (London) **415**, 614 (2002).

[37] P. N. Segre, F. Liu, P. Umbanhowar, and D. A. Weitz, Nature (London) **409**, 594 (2001).
[38] R. Kono, J. Phys. Soc. Jpn. **15**, 718 (1960).
[39] C. A. Bero and D. J. Plazek, J. Polym. Sci., Part B: Polym. Phys. **29**, 39 (1991).
[40] C. M. Roland, S. Hensel-Bielowka, M. Paluch, and R. Casalini, Rep. Prog. Phys. **68**, 1405 (2005).
[41] M. Paluch, C. M. Roland, R. Casalini, G. Meier, and A. Patkowski, J. Chem. Phys. **118**, 4578 (2003).
[42] E. R. Weeks and D. A. Weitz, Phys. Rev. Lett. **89**, 095704 (2002).
[43] http://www.sidrich.com/carbon/summary.htm